Wave-vector space picture for radiationless focusing and beaming

Varat Intaraprasonk[1] and Shanhui Fan[2,*]

[1]*Department of Applied Physics, Stanford University, Stanford, California 94305, USA*
[2]*Department of Electrical Engineering, Stanford University, Stanford, California 94305, USA*
**Corresponding author: shanhui@stanford.edu*

Received June 18, 2009; accepted July 24, 2009;
posted September 2, 2009 (Doc. ID 113063); published September 24, 2009

Radiationless interference of an electromagnetic wave occurs in the near field when the feature sizes of the waves are at the deep subwavelength scale. We present the propagation in such a regime using a wave-vector space picture. Using this picture, we reproduce the condition to achieve near-field focusing. We also design the initial field distribution needed for near-field beaming, where an intensity distribution maintains its shape as it propagates. We conclude the discussion by proposing a possible implementation of the near-field beaming scheme. © 2009 Optical Society of America

OCIS codes: 070.7345, 240.0240.

Interference is at the heart of many electromagnetic effects. Although most interference experiments have been carried out in the far field, there have been recent theories and experiments pointing out interesting interference effects in the near field. In particular, Merlin *et al.* [1–3] showed that such "radiationless interference" can be exploited to create deep subwavelength focusing. In this Letter, we provide a description of near-field interference based on wave-vector space arguments, which provide additional insight to the near-field focusing effect. We also point out a near-field beaming effect and discuss its possible experimental implementation.

In near-field interference, one specifies the field (F) at the plane $z=0$ and calculates the field at other planes z. For this purpose, we represent $F(y,z)$ in wave-vector space as

$$F(y,z)=\frac{1}{\sqrt{2\pi}}\int \tilde{F}(k_y,z)\exp(ik_y y)\mathrm{d}k_y. \tag{1}$$

The connection between $F(y,z)$ and $F(y,z=0)$ is then straightforwardly calculated in the wave-vector space, noting that

$$\tilde{F}(k_y,z)=\tilde{F}(k_y,0)\exp(ik_z(k_y)z)\equiv\tilde{F}(k_y,0)T(k_y,z), \tag{2}$$

where we define the transfer function $T(k_y,z)\equiv\exp(ik_z(k_y)z)$. In general, $k_z^2+k_y^2=(n\omega/c)^2\equiv k_0^2$, where n is the index of refraction of the material, ω is the angular frequency, and c is the speed of light. In the near-field regime, however, following [1–3] one is typically concerned with the initial field distribution $F(y,0)$ that has most of its features in the deep subwavelength regime. Thus most of the relevant k_y components of $\tilde{F}(k_y,0)$ satisfy $k_y\gg k_0$, giving

$$k_z\approx ik_y. \tag{3}$$

Thus, $T(k_y,z)\approx\exp(-k_y z)$ (light line, Fig. 1). Equation (2) can be approximated as

$$\tilde{F}(k_y,z)=\tilde{F}(k_y,0)\exp(-k_y z). \tag{4}$$

Using this formula, we now discuss focusing and beaming effects in the near field.

In near-field focusing, the goal is to focus the electromagnetic beam into a deep subwavelength spot. Following [1], at the focal length $z=L$, a focal spot size on the order of $l=2\pi/q_0$ corresponds to a flat spectrum in wave-vector space up to $k_y=q_0$. To get such a flat spectrum, noting the specific form of $T(k_y,L)=\exp(-k_y L)$, one can simply choose $\tilde{F}(k_y,0)$ in the region $0<k_y<q_0$ to be (dark line, Fig. 1)

$$\tilde{F}(k_y,0)=\exp(+k_y L), \tag{5}$$

giving (dotted curve, Fig. 1)

$$\tilde{F}(k_y,L)=\tilde{F}(k_y,0)\exp(-k_y L)=\text{const}. \tag{6}$$

Such a flat spectrum occurs only at $z=L$. For $k_y>q_0$, we simply choose $\tilde{F}(k_y,0)$ to be symmetric around q_0.

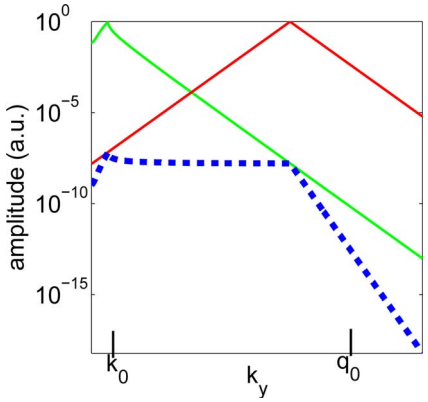

Fig. 1. (Color online) Focusing occurs when the field spectrum in wave-vector space $\tilde{F}(k_y,L)$ (dotted curve) becomes flat. This occurs at $z=L$, where the exponentially growing part of $\tilde{F}(k_y,0)$ (dark line) cancels with the exponentially decaying part of $T(k_y,L)$ (light line).

As a result,

$$\tilde{F}(k_y,0) = \exp(-|k_y - q_0|L), \tag{7}$$

which corresponds to

$$F(y,0) = \frac{L\exp(iq_0y)}{\pi}\frac{}{y^2+L^2}. \tag{8}$$

In Eq. (8), the Lorentzian envelope $(y^2+L^2)^{-1}$ provides the exponential growth in wave-vector space needed for focusing, while the oscillating function $\exp(iq_0y)$ shifts the center spatial frequency to $k_y = q_0$. This reproduces exactly the result in [1,4]. The wave-vector space interpretation, however, provides a somewhat more intuitive picture on the choice of the form of the initial field.

Next, we propose to follow similar steps to achieve deep subwavelength near-field beaming. By beaming, we aim to maintain a constant beam envelope as an electromagnetic beam propagates over a range of z. Because $T(k_y,z)$ is an exponentially decaying function in the k_y space, we choose $\tilde{F}(k_y,0)$ to be a Gaussian (Fig. 2a), with the center spatial frequency $q_0 \gg k_0$, i.e.,

$$F(y,0) = \exp(iq_0y)\exp\left(-\frac{y^2}{2\sigma}\right). \tag{9}$$

Hence,

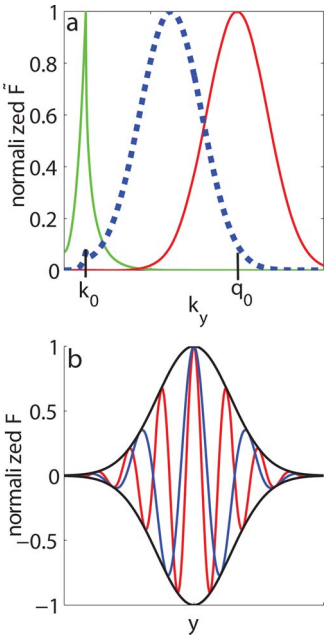

Fig. 2. (Color online) a, Near-field beaming scheme in wave-vector space. Beaming occurs when $\tilde{F}(k_y,z)$ (dotted curve), which is the product of the Gaussian $\tilde{F}(k_y,0)$ (dark curve) and $T(k_y,z)$ (light curve), maintains the shape and width as z increases. b, Real part of the field in position space. It maintains the same Gaussian envelope (dark curve), but the spatial oscillation of $F(k_y,z)$ [dark gray (blue online) curve] has a longer period than that of $F(k_y,0)$ [light gray (red online) curve].

$$\tilde{F}(k_y,0) = \sqrt{2\pi\sigma}\exp\left(-\frac{\sigma}{2}(k_y - q_0)^2\right). \tag{10}$$

Then using Eq. (4), we have

$$\tilde{F}(k_y,z) = \sqrt{2\pi\sigma}\exp\left(-zq_0 + \frac{z^2}{2\sigma}\right) \times\exp\left(-\frac{\sigma}{2}\left(k_y - \left(q_0 - \frac{z}{\sigma}\right)\right)^2\right), \tag{11}$$

$$F(y,z) = \exp\left(-zq_0 + \frac{z^2}{2\sigma}\right)\exp\left(i\left(q_0 - \frac{z}{\sigma}\right)y\right) \times\exp\left(-\frac{y^2}{2\sigma}\right). \tag{12}$$

We can see that the envelope remains Gaussian with same width for any z, achieving the beaming effect as desired (Fig. 2).

In general, the beaming effect persists only for a finite range of z, and here we calculate the maximum distance z_{max} that the beam can propagate without distortion. There are two effects that limit the propagating distance. First, the center spatial frequency $q(z)$ of the Gaussian shifts lower at a constant rate $q(z)=q_0-z/\sigma$, but Eq. (3) is true only when $q(z)>k_0$. By solving for z_{max}, which makes the center spatial frequency drop below k_0, we get

$$z_{max} \approx (q_0 - k_0)\sigma. \tag{13}$$

Second, the amplitude of the Gaussian decays exponentially in z, which is characteristic of any evanes-

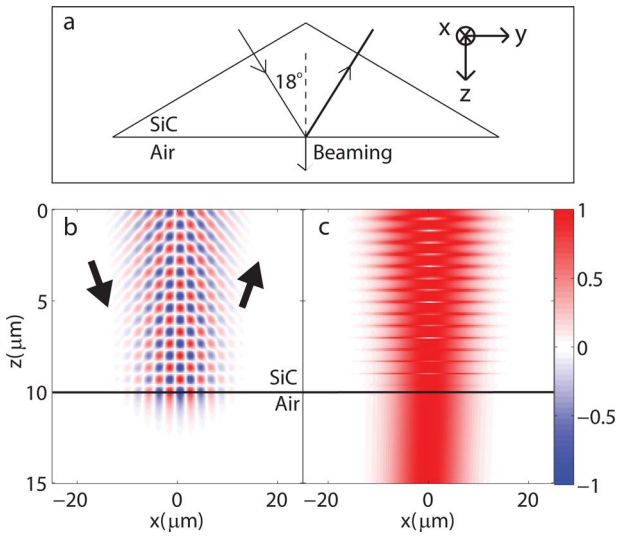

Fig. 3. (Color online) Beaming scheme using a TM-polarized Gaussian beam incident at an oblique angle inside an SiC prism. The wave undergoes total internal refraction and gives an evanescent wave with a Gaussian profile on the air side. Arrows in a and b show the direction of incident and reflected waves. b, Real part of E_x; c, absolute value of E_x, normalized such that in each plane of constant z, the maximum amplitude is 1 to emphasize the constant Gaussian envelope.

cent wave. That means at large z, the Gaussian envelope can decay below, and get dominated by, the very small wave-vector component in the propagating region $k_y < q_0$, which does not decay in z. We can solve for this limit in $z_{\max}$ by setting the decayed amplitude of the Gaussian equal to the value of the wave-vector component at $k_y = k_0$,

$$\exp\left(-zq_0 + \frac{z^2}{2\sigma}\right) = \exp(-\sigma(k_0 - q_0)^2/2), \quad (14)$$

which gives

$$z_{\max} = q_0\sigma(1 - \sqrt{1 - (1 - k_0/q_0)^2}). \quad (15)$$

Notice that if $q_0 \gg k_0$, both $z_{\max}$ from Eqs. (13) and (15) converge to

$$z_{\max} = q_0\sigma. \quad (16)$$

We now do the analysis for general shapes of input beams with the form $F(y,0) \equiv M(y)\exp(iq_0y)$, with $M(y)$ symmetric and real. For simplicity, assume the normalization $\tilde{M}(0) = 1$. We can find the rate that the center spatial frequency shifts initially using the first-order Taylor expansion to be

$$\frac{dq}{dz} = \frac{1}{\tilde{M}''(0)}. \quad (17)$$

We can estimate the range $z_{\max}$ that the wave can propagate before the evanescent part is dominated by the propagating part,

$$z_{\max} = \frac{q_0}{q_0^2 - 2k_0^2}\log\left(\frac{1}{\tilde{M}(q_0 - k_0)}\right). \quad (18)$$

This approximation assumes that the center spatial frequency does not shift significantly.

The FWHM (W) of $\tilde{F}$ changes as z increases. We find that the change in the FWHM is constant to first order ($dW/dz = 0$). The second-order change is

$$\frac{1}{2}\frac{d^2W}{dz^2} = -\frac{1}{\tilde{M}'\left(\frac{W}{2}\right)}\left\{\frac{1}{\tilde{M}''(0)} - \frac{W}{2}\frac{1}{\tilde{M}'\left(\frac{W}{2}\right)} - \frac{W^2}{4}\left(1 - \frac{\tilde{M}''\left(\frac{W}{2}\right)}{2\left(\tilde{M}'\left(\frac{W}{2}\right)^2\right)}\right)\right\}. \quad (19)$$

As expected, by setting M to be Gaussian, we get $dW = 0$, which is required for beaming.

We propose an experimental implementation of the near-field beaming scheme by shining a Gaussian beam into an SiC prism. The beam hits the bottom SiC–air interface at an oblique angle, as shown in Fig. 3. The polarization is chosen to be TM, so the field F refers to E_x. We choose the material to be SiC at $f = 23.4$ THz; at this frequency $n_{\mathrm{SiC}} = 10.3$ [5]. The beam width is $\sqrt{\sigma} = 5$ μm, and the incident angle is 18°. The incidence angle is chosen such that the center spatial frequency $q_0 (= 1.5 \times 10^6\ \mathrm{m}^{-1})$ at the bottom SiC–air interface is much greater than $k_{0(\mathrm{air})}$ $(= 0.5 \times 10^6\ \mathrm{m}^{-1})$. The large index of SiC at this frequency ensures that such spatial frequency still propagates in SiC. The beam undergoes total internal reflection at the SiC–air interface, giving an oscillating Gaussian beam on the air side; the Gaussian beam input gives the factor $\exp(-y^2/2\sigma)$, while the oblique angle gives the oscillation $\exp(iq_0y)$. This beam then undergoes beaming in the air region. We can see in Fig. 3 that the beam in air indeed maintains the same amplitude envelope, and the amplitude variation in the z direction in fact agrees well with Eq. (12).

This work is supported in part by U.S. Air Force Office of Scientific Research (AFOSR) (FA 9550-08-1-0407). V. Intaraprasonk is supported by a Stanford Graduate Fellowship.

References

1. R. Merlin, Science **317**, 927 (2007).
2. A. Grbic, L. Jiang, and R. Merlin, Science **320**, 511 (2008).
3. A. Grbic, and R. Merlin, IEEE Trans. Antennas Propag. **56**, 3159 (2008).
4. L. E. Helseth, Opt. Commun. **281**, 1981 (2008).
5. E. D. Palik, ed., *Handbook of Optical Constants of Solids* (Academic, 1985).